

UC Davis

UC Davis Previously Published Works

Title

Sex-specific evolution of relative leg size in *Drosophila prolongata* results from changes in the intersegmental coordination of tissue growth

Permalink

<https://escholarship.org/uc/item/31k1s05q>

Journal

Evolution, 73(11)

ISSN

0014-3820

Authors

Luecke, David Michael
Kopp, Artyom

Publication Date

2019-11-01

DOI

10.1111/evo.13847

Peer reviewed



Published in final edited form as:

Evolution. 2019 November ; 73(11): 2281–2294. doi:10.1111/evo.13847.

Sex-specific evolution of relative leg size in *Drosophila prolongata* results from changes in the intersegmental coordination of tissue growth:

Tissue growth and limb size evolution

David Michael Luecke^{1,2}, Artyom Kopp¹

¹Department of Evolution and Ecology, University of California – Davis

²Current Address: Department of Integrative Biology, Michigan State University

Abstract

Evolution of relative organ size is the most prolific source of morphological diversity, yet the underlying molecular mechanisms that modify growth control are largely unknown. Models where organ proportions have undergone recent evolutionary changes hold the greatest promise for understanding this process. Uniquely among *Drosophila* species, *D. prolongata* displays a dramatic, male-specific increase in the size of its forelegs relative to other legs. By comparing leg development between males and females of *D. prolongata* and its closest relative *D. carrolli*, we show that the exaggerated male forelegs are produced by a sex- and segment-specific increase in mitosis during the final larval instar. Intersegmental compensatory control, where smaller leg primordia grow at a faster rate, is observed in both species and sexes. However, the equilibrium growth rates that determine the final relative proportion between the first and second legs have shifted in male *D. prolongata* compared both to conspecific females and to *D. carrolli*. We suggest that the observed developmental changes that produce new adult proportions reflect an interplay between conserved growth coordination mechanisms and evolving organ-specific growth targets.

Keywords

Growth; Shape; Allometry; Sexual Dimorphism; *Drosophila prolongata*

Introduction

How the immense phenotypic diversity seen in life on earth is produced by selective manipulation of genetic variation is the central question of evolutionary biology. Novel structures occasionally arise and beget subsequent diversification, but the most common mode of evolution is modification of existing body parts. The most prolific mechanism of

dluecke@ucdavis.edu, akopp@ucdavis.edu.

Author contributions

DL conceived the project, designed experiments, performed and oversaw data collection, performed data analysis, and wrote the initial draft of this manuscript. AK guided experimental design, contributed stocks, materials and expertise, assisted in analysis design, and reviewed and revised the manuscript.

Data Accessibility Statement: Data and analysis scripts are available on Dryad doi:10.25338/B8303J.

morphological diversification involves changes in the relative sizes of tissues and organs (Huxley 1932; Gould 1966; Stern and Emlen 1999; Mirth et al. 2016). This type of change not only modifies existing traits, but can also produce organs capable of novel functions ('character transformation' (Wagner and Lynch 2010)). Understanding this process is crucial for explaining the origin of phenotypic diversity at the genetic and cellular level.

Changes in the relative sizes of body parts require modification of the developmental mechanisms of growth control, which integrate cell specification, growth, division and death, and respond to cues from the rest of the developing organism while preventing genetic and environmental variability from disrupting the production of functional adult traits (Tumaneng et al. 2012; Irvine and Harvey 2015). The intricacies of growth control remain, even after considerable progress over decades of research, a major enigma in developmental biology (Shingleton and Frankino 2018). The robustness of development in the face of ongoing perturbations requires well-buffered control mechanisms (canalized pathways *sensu* (Waddington C.H. 1942)), and organ size and shape show all the hallmark features of developmental buffering (Breuker et al. 2006). Evolutionary changes in relative proportions must therefore modify these buffered systems of size regulation without undermining developmental robustness or disrupting any of the selectively constrained organ functions. Yet the extensive diversity in relative organ size shows that evolution can change the outcomes of growth control with apparent ease (Voje et al. n.d.; Lavine et al. 2015). Standing in stark contrast to the ubiquity of this mode of morphological evolution, the underlying developmental and molecular changes are largely unknown.

Insect models including *Drosophila melanogaster* and tobacco hornworm *Manduca sexta* have provided much of the growing knowledge of the roles played by various signaling molecules in controlling tissue growth (Nijhout and Grunert 2010; Mirth and Shingleton 2012; Andersen et al. 2013). Similarly, the horns of *Trypoxylus* and *Onthophagus* beetles have enabled the most complete molecular dissection of organ size evolution to date (Wasik et al. 2010; Emlen et al. 2012; Ito et al. 2013). These examples show the power of experimentally tractable insect models to address the fundamental processes at play in the diversification of animal shapes. Analysis of natural variation in organ size within and between species can produce insights into the developmental control of tissue growth and show how development evolves to produce structures that change in size but retain functionality, be it ancestral or a novel function enabled by the shift in relative size.

Drosophila prolongata, a close relative to the model species *D. melanogaster*, shows a slew of recently evolved sexually dimorphic traits (Singh and Gupta 1977). The most noticeable of these is a dramatic increase in the relative size of male forelegs (Fig. 1). These exceptionally large legs are used for male-male grappling, displaying to females, and for the novel courtship behavior of leg vibration, suggesting that they evolve under sexual selection (Setoguchi et al. 2014). The size increase is segment- and sex-specific and is not observed in any other species including sister species *D. carrolli* (Gompel and Kopp 2018), indicating a recent evolutionary change in both sexual dimorphism and within-sex allometry. In other words, developmental mechanisms controlling leg growth must differ both between the forelegs and the other leg pairs, and between the forelegs of males and females, and these

differences have evolved after the divergence of *D. prolongata* from its sibling species (Fig. 1, 2).

In this study, we compare leg development between segments, sexes, and species to identify the cellular processes that were modified in the course of evolution to produce the derived leg proportions, and to explore how serially homologous structures respond to dramatic shifts in relative size. We show that sex- and segment-specific increase in leg size is achieved through changes in the rate of cell division, even while maintaining a buffered system of compensatory growth between segments. This dynamic suggests that evolution has targeted the organ's intrinsic size (*sensu* (Bryant and Simpson 1984)), and that developmental changes result from the response of conserved growth coordination mechanisms to the altered organ-specific growth targets.

Materials and Methods

Fly Stocks

The following strains were used: *D. prolongata* BaVi043 (collected by H. Takamori, in BaVi, Vietnam March 2005); *D. carrolli* KB866 (collected by A. Kopp and O. Barmina in Kuala Belalong, Brunei, October 2003); *D. rhopaloa* BaVi067 (H. Takamori, BaVi, Vietnam March 2005); *D. fuyamai* KB1217 (A. Kopp and O. Barmina, Kuala Belalong, Brunei, October 2003); *D. elegans* (14027–0461.00, US *Drosophila* species stock center), and *D. immigrans* and *D. melanogaster* (A. Kopp, Winters CA, collected prior to 2010).

Adult Leg Measurements

Adult flies were anesthetized on a carbon dioxide pad, sexed, and dissected under a stereoscope. The wings and first and second leg pairs were removed from the body and all parts were arranged onto tape adhered adhesive-side up on an index card. The collection of body and appendages from each individual was imaged under the dissecting microscope using a Leica camera attachment. Leg and thorax lengths were then measured using the ObjectJ plugin (sils.fnwi.uva.nl/bcb/objectj/index.html) in ImageJ (Schneider et al. 2012). Leg length was taken as the full path length from claw to the base of the coxa. Thorax length was taken as the straight line distance from the anterior edge of the mesothorax to the tip of the scutellum. Data analysis was carried out in R. The two leg measurements for each segment were averaged, then the ratio and log ratio of leg lengths was compared by pairwise t-test between males of all species, females of all species, and between sexes within each species. The Smatr3 package (Warton et al. 2012) was used for estimation of allometric parameters by log transformation of the trait data, then estimation of the slope and intercept parameters of a linear relationship between the log of leg length and the log of thorax length by standard major axis regression.

Embryo collection, staining, mounting, and image analysis

Most species do not lay eggs as readily as *D. melanogaster*, so the egg collection protocol was modified from standard methods to maximize the number of eggs at the expense of highly synchronized embryos. High densities of flies were placed in empty bottles with air holes poked into the sides for ventilation and folded filter paper for habitat structure. A

grape agar plate with splotches of thick yeast paste was taped onto the top to provide a substrate for laying eggs. This setup was maintained for a day to train the flies, then left overnight with a fresh plate laying on a wet tissue to prevent desiccation. In the morning, a new plate was provided and left for two hours. Both the overnight and morning plate were kept at 25 C for 5 hours after removal to allow the youngest embryos to develop, then removed from the plate with a paint brush and squirt bottle of distilled water. The embryo collection was thus of varying age, with the youngest embryos 5 hours old. Embryos were fixed and stained by standard protocols with the primary antibodies mouse anti-Dll (Duncan et al. 1998) at 1:1000 and rabbit anti-Msl2 ((Coppes et al. 1998), kindly provided by Dr. Mitzi Kuroda) at 1:100, and the secondary antibodies FITC anti-mouse and Texas Red anti-rabbit, both at 1:200. After staining, the embryos were arranged with a wet paint brush on a clean glass slide so the dorsal side was facing up, then transferred to a pre-treated poly-lysine slide by placing the second slide flush against the embryos, adhering the dorsal sides to the glass. The embryos were then covered in Fluoromount-G (SouthernBiotech) and had a coverslip gently rolled over the ventral sides. This arrangement enables the simultaneous imaging of all 6 leg primordia on the ventral surface. Line-sequence 2 channel Z-stacks were taken on an Olympus FluoView 1000 confocal microscope with the 60x objective, capturing the full depth of the T1 and T2 leg primordia. The cells in each Dll-positive cluster were counted using the ImageJ Multi-point tool (Schneider et al. 2012), then the Msl2 channel was used to identify the sex of the embryo.

Statistical analysis was carried out in R. The two cell counts for each segment were averaged, and contributions of sex, species, and the sex by species interaction to the difference in cells between T1 and T2 segments was tested by ANOVA.

Staging and Sexing Larvae

To stage larvae from the onset of 3rd instar (L3), larvae and food were spooned from 4–5 day old high-density bottle cultures and put into a petri dish, which was flooded with distilled water so larvae could be removed. Larvae were sorted on a glass well dish under a stereoscope with a fine paintbrush. Larval instar was determined by mouthpart morphology, trachea morphology, and size. 1st and 2nd instar larvae (L1 and L2) were placed into food vials and kept at 26 C. After 24 hours larvae were again sorted, and all 3rd instar larvae were removed and put into vials at densities between 5 and 10 individuals, comprising a “new L3 +/- 12 hour” set. The food in these vials was agitated with a wet paint brush to assist the larvae in forming a healthy culture. These vials were kept at 26 C until the larvae were sexed and dissected.

To stage larvae from egg laying, a high density of flies were allowed to lay eggs in a bottle for 24 hours, then removed. These bottles were kept at 26 C until the appropriate time point, at which point larvae were removed by the same method. Most of the larvae were thus older than the identified time, but relative age comparisons will still hold. Larvae were sexed immediately prior to dissection. Males and females were separated based on the presence or absence of testes by viewing larvae under a stereoscope on a glass plate over a black background. They were kept in separate wells in distilled water until dissection.

Larval Disc Dissection, Fixation, Immunohistochemistry, and Slide Preparation

Larvae were placed on an index card and cut in half with a razor blade. The anterior half was moved with forceps to 1x PBS and inverted by placing the tips of one pair of forceps into the body cavity while pressing on the head with the tips of a second pair of forceps, causing the cuticle to invert and roll up the second pair of forceps. This maneuver is done with the dorsal side down, so scraping of the forceps does not disturb the imaginal discs. The inverted anterior halves were moved in 700uL PBS to a 1.5mL microcentrifuge tube, to which 100uL 32% paraformaldehyde was added (final concentration 4%), and rocked at room temperature for 30 minutes. After fixation, the tissue was washed 3x for 15 minutes with 1x PBS, then stored at 4C in PBS until secondary dissection. Prior to secondary dissection, fixed tissue was washed 3x for 15 minutes at room temperature in either TNT (0.1M Tris-HCl, 0.3M NaCl, 0.5% Triton X-100, pH 7.4) for pH3 solo stains, or Blocking Buffer (1x PBS, 5% Normal Goat Serum, 0.3% Triton X-100) for pH3/Dcp-1 counterstains, as we found that the anti-Dcp1 stain worked better in PBS-based buffer.

During secondary dissection the gut, salivary glands, and any remaining fat body or other loose tissues were removed, leaving behind a cleaned body wall with the T1 and T2 leg disc pairs held together by the CNS still attached by disc-wall connections and the larval mouth hooks. These cleaned body walls were transferred back into microcentrifuge tubes for blocking and staining. All tissue was blocked for 30 minutes at room temperature in Image-iT FX Signal Enhancer (Invitrogen), then washed 3x for 15 minutes at room temperature in the same buffer as before dissection. Cell division was marked with either Phospho-Histone H3 (Ser10) Antibody (#9701, Rabbit) for solo stains, or Phospho-Histone H3 (Ser10) (6G3) Antibody (#9706, Mouse) for apoptosis counterstains, while apoptosis was marked with Cleaved Drosophila Dcp-1 (Asp216) Antibody (#9578, Rabbit), all from Cell Signaling Technology. All primary antibodies were diluted 1:100 in either TNT for solo pH3 stains or Antibody Dilution Buffer (1x PBS, 1% BSA, 0.3% Triton X-100) for pH3/Dcp-1 counterstains. Tissue was submerged in primary antibody solution and left rocking overnight at 4C. Primary antibody was removed, and tissue was washed 6x for 15 minutes at room temperature in either TNT for the single pH3 stain, or PBS-Tr (0.1% Triton X-100 in PBS) for the double stain. Tissue was then submerged in 50 uL secondary antibody and left rocking in the dark for either 4 hours at room temperature or overnight at 4 C. Secondary antibodies used were goat FITC anti-mouse and goat Texas Red anti-rabbit (Invitrogen), both at 1:200 in either TNT (solo pH3) or Antibody Dilution Buffer (pH3/Dcp-1 counter). At the end of the secondary incubation time, 1 uL of 100 ug/mL DAPI (final concentration 2 ug/mL) was added to the secondary antibody buffer and incubated for an additional 10 minutes at room temperature in the dark. Tissue was then washed in TNT or PBS-Tr (as before) 6x for 15 minutes at room temperature in the dark, then transferred to a depression glass well for final dissection and mounting. The mouth hooks were separated from the CNS, and the connections between discs and body wall were clipped by forceps, then the brain was severed from the thoracic ganglion. The discs and ganglion were transferred to a drop of PBS on a poly-lysine treated slide, placed so the dorsal side of the ganglion adhered first to the glass, then the discs were spread flat onto the glass surrounding the ganglion. The PBS was removed and replaced by Fluoromount-G (SouthernBiotech), and a cover slip was rolled onto the tissue.

Disc Image Analysis

Images were collected on an Olympus FluoView 1000 confocal microscope with a 20x objective as line-sequential multi-channel images in a single plane that represented each disc's surface. These images were converted to inverted greyscale 8-bit tif files for analysis with the Image-based Tool for Counting Nuclei (ITCN, imagej.nih.gov/ij/plugins/itcn.html) in ImageJ (Schneider et al. 2012) and FIJI (Schindelin et al. 2012). The ImageJ freehand trace tool was used to measure total disc size and identify the boundaries for ITCN cell counting. Variation in stain strength and quality required variation in ITCN parameters, which were adjusted based on visual inspection of identified nuclei, however parameter values remained constant across all discs for each individual.

Statistical analyses were carried out in R. For each disc, the average cell size was calculated as the total disc area divided by the number of cells; the mitotic index (MI) was calculated as the number of pH3-positive cells divided by the number of DAPI-stained nuclei; and the apoptotic index (AI) as the number of Dcp-1-positive cells divided by DAPI-stained nuclei. If measurements from both discs were available, the values for disc area, the number of DAPI-stained nuclei, calculated cell size, pH3 and Dcp-1 stained cells, and the calculated MI and AI values were averaged between the two discs of each segment to give T1 and T2 values for that individual. These segmental values were then used to calculate the attributes of individual larva for analyses reported in Results, see Figure 3 legend for details. Timepoints measured in days after egg laying and those measured in hours after molt to L3 instar were both converted to percent larval development by taking observed average lengths of larval development for each sex and species (6.7, 7.0, 7.2, and 8.1 days for female *D. carrolli*, male *D. carrolli*, female *D. prolongata*, and male *D. prolongata* respectively), and assuming the molt to 3rd instar takes place halfway through larval development. This agrees with our empirical observations of the time after egg laying when L3 larva are first observed and the ages reached by the 3rd instar-staged vials before pupariation.

Results

***D. prolongata* has exceptionally long male front legs and novel sexual dimorphism in leg proportions**

To place the relative leg sizes in an evolutionary context, we chose six additional *Drosophila* species that represent a variety of body sizes and degrees of relatedness to *D. prolongata* (Figure 2). Male *D. prolongata* have trait values that stand out from the trends observed in the other species. The first legs of males are by far the longest, even accounting for the trend of larger flies having longer legs (Figure 2A). Comparing the legs of male *D. prolongata* to those of male *D. immigrans*, which has a similar body size, shows the disproportional length of the male foreleg in *D. prolongata*.

The increase in male foreleg size in *D. prolongata* is also accompanied by more subtle changes in homologous organs. The male second leg is also longer relative to body size than in other species, as is the female foreleg (but, interestingly, not the female second leg). The relationship between first and second legs can be visualized by plotting the ratio of their lengths, with values >1 indicating individuals with longer first than second legs (Figure 2B).

This ratio has evolved drastically in *D. prolongata*, reaching 1.05 in females and 1.29 in males, well outside the range of 0.92 to 1.01 in the six outgroup species. These values clearly show that *D. prolongata* has evolved a novel sexual dimorphism in relative leg size – it is the only species in which this ratio shows significant difference between sexes after multiple test correction (*D. prolongata*: Holm's $p=2.67e-14$; *D. immigrans*: $p=0.242$).

Considering these traits in a phylogenetic context shows no trend toward exceptional foreleg size or sexual dimorphism over long evolutionary time – *D. prolongata* is just as diverged from its closest sister species as from more distantly related outgroups. Evolutionary changes that produced the sexual dimorphism have occurred recently, since the split from the lineage leading to *D. rhopaloa* and *D. carrolli*. To investigate how this novel dimorphism arose, we characterized leg development in males and females of *D. prolongata* and *D. carrolli*.

The size of embryonic leg primordia reflects species divergence but not sexual dimorphism

Fly legs begin their development as clusters of embryonic cells. These primordial leg tissues become segregated from larval tissue in structures known as imaginal discs (Held 1995). The growth of future legs occurs primarily in these discs during the larval stage. The end of the larval stages and the onset of pupariation is a critical developmental time point for holometabolous insects. In *Drosophila*, it occurs as a morphologically obvious stage, the white prepupa, and represents a homologous developmental marker between sexes and species. At this stage, the imaginal discs have largely completed their growth and are beginning the metamorphosis into their respective adult structures.

To test whether the differences in leg size are initiated at the embryonic stage, we measured the sizes of embryonic leg primordia by staining mid-to-late stage embryos with an antibody against *Distalless*, which marks each set of leg primordia in a stereotypic pattern. Legs at this stage are easily identified as six cell clusters arranged in pairs along the anterior-posterior axis, near the head on the ventral surface. Embryos were sexed by staining with an antibody against Msl-2, a male-specific protein involved in dosage compensation. In the embryonic limb primordia, for both cell count difference and cell count ratio (not shown), there is a significant effect of species but not sex, with both sexes of *D. prolongata* having slightly higher T1 - T2 size differences compared to the sister species *D. carrolli* (Figure 3A). This difference is consistent with the increase in first to second leg length ratio in female *D. prolongata* (Figure 2B), but does not explain the sexual dimorphism in the limbs' relative size. We next investigated whether the sexual dimorphism in the T1 – T2 size difference is established during the larval growth of these discs.

Sexually dimorphic intersegmental difference in cell number is present by the end of larval development

We used the morphologically distinct developmental timepoint of the white prepupa to investigate whether organ size difference is established during the growth of imaginal discs. We estimated the number of cells per T1 and T2 leg disc from sexed white prepupa of *D. prolongata* and *D. carrolli* by staining them with DAPI and imaging on a confocal

microscope. The discs of each individual were kept together, allowing us to quantify the difference between segments for each individual, rather than comparing average T1 and T2 values. In the white prepupal discs (Figure 3A'), there are significant effects of species, sex, and their interaction on the difference in cell number between T1 and T2. We further tested for sexual dimorphism within each species, finding no significant difference between male and female *D. carrolli* but a significant difference between male and female *D. prolongata* even after downsampling each species to the smallest sample size from *D. carrolli* and adjusting for multiple tests. Finally, the difference in cell number between T1 and T2 discs is not significantly different from 0 in either sex of *D. carrolli* or in female *D. prolongata*, but is significantly positive in male *D. prolongata*, again after downsampling and adjusting for multiple tests. These results show the novel dimorphism in relative leg size has been generated by the end of larval development, at which point the intersegmental difference in the number of cells mirrors the difference in leg size observed in adult flies (Figure 2). *D. prolongata* males have on average 16% more cells in their front leg discs, while the female T1 discs are only 2% larger than their T2 counterparts. In *D. carrolli*, white prepupa of both sexes have similar numbers of cells in T1 and T2 leg discs. Cell size does not appear to be different between the two segments in either species or sex. Combined with the lack of sexual dimorphism in the size of embryonic leg primordia, these data indicate that the development of size differences between T1 and T2 legs is mediated by changes to the relative rates of cell proliferation in the two segments during the larval growth period. We next constructed a developmental time series to determine the timing of this change.

Segment size begins diverging early in the 3rd larval instar

We collected 3rd instar larva of various ages, timed either from egg laying or from molting to 3rd instar, and measured the number of cells in the first and second leg discs for individual larva by staining for DAPI and imaging on a confocal microscope. The growth trajectories of T1 and T2 discs across this period of development show a trend where T1 appears to become gradually larger than T2 in *D. prolongata* males, but not in females or in *D. carrolli* (Supplemental Figure 1). Size variation is high within each species and sex, and the slopes of the growth curves calculated from aggregate data are not statistically significant (Supplemental Figure 1). Instead, we used paired measurements of T1 and T2 discs from the same individuals to calculate the difference in cell number between segments for each larva. We found that in *D. prolongata* males, the youngest 3rd instar larvae have more similarly sized T1 and T2 leg discs than the older 3rd instar larvae (Figure 3D, bottom), and that only male *D. prolongata* show a positive slope in the difference between cell numbers in T1 and T2 leg discs over the third instar (linear model $F=41.5$, $p=2.4e-9$, Figure 3B). We also see a small but persistent segment size difference favoring T1 discs in female *D. prolongata* larvae, consistent both with the measurements of embryonic leg primordia and with adult leg sizes; however, this difference is constant over time. Thus, the major developmental dimorphism in this species is the increasing difference in cell number between the T1 and T2 leg discs in males over the course of the 3rd larval instar. We next sought to identify the cellular mechanisms that produce the elevated rate of growth seen in the first leg disc of male *D. prolongata*.

Segment-specific increase in mitosis co-occurs with the appearance of size divergence

To track the amounts of cell proliferation and apoptosis during development, we stained discs from staged individuals with antibodies specific to protein modifications exhibited during cell division (Histone H3 phosphorylated at serine 10) or programmed cell death (cleaved Caspase-1). As with DAPI cell counts, all four T1 and T2 leg discs from each larva were stained and processed together, allowing us to measure the relative amounts of cell division and programmed cell death occurring in each individual. *D. prolongata* displays a species-specific sexual dimorphism in the relative amount of mitotic cells in T1 compared to T2 leg discs (Figure 3C). We find significant effects of both species and sex on the bias of mitosis towards T1, and the number of excess mitotic cells in larval T1 discs is sexually dimorphic in *D. prolongata* but not in *D. carrolli* (Figure 3C). These results show that there is a greater rate of mitosis in T1 discs relative to T2 discs in male *D. prolongata*.

Interestingly this male-specific bias towards T1 mitosis is temporally constrained to a relatively brief time during the third instar (Figure 3D, top), which occurs at the same time as the initial emergence of intersegmental size divergence during the larval development of male *D. prolongata* (Figure 3D). In contrast to mitosis, there is no sexual dimorphism in the relative levels of apoptosis between segments, and in fact all differences are in the opposite direction compared to what would produce larger first legs in male *D. prolongata* (Figure 3C'). Taken together, these results indicate that the increased size of first relative to second legs in male *D. prolongata* is produced by increased cell division in first compared to second leg discs during the 3rd larval instar.

Relative size of leg primordia evolves while maintaining compensatory growth between segments

In many insects, both hemimetabolous and holometabolous, organ growth is influenced by the condition of the other organs in the body (O'Farrell and Stock 1953; Kunkel 1977; Nijhout and Emlen 1998; Stieper et al. 2008). *Drosophila* discs in particular have been shown to compensate for changes in the growth rates of other discs in the individual by modifying their own growth (Parker and Shingleton 2011). This phenomenon has generally been considered in the context of wound healing and growth retardation. We decided to test whether similar dynamics contribute to the lability of relative organ sizes during evolution.

To investigate whether growth compensation is taking place in the developing legs of *D. prolongata* and *D. carrolli*, we looked for a relationship between the ratio of leg sizes, measured by cell number, and the difference in their growth rates, measured as the mitotic index (MI, the proportion of cells undergoing mitosis), across the full set of discs from all time points. We reasoned that a compensatory dynamic would result in higher growth in smaller discs and lower growth in larger discs (Figure 4A), and thus cause individuals with higher T1/T2 size ratio to adjust the relative rates of cell proliferation toward a lower T1 – T2 MI difference (more growth in T2), and *vice versa*. In other words, this predicts a negative correlation between the ratio of disc cell counts and the intersegmental difference in MIs. The point where this relationship crosses from higher T1 growth to higher T2 growth represents the “target” ratio of leg sizes; outside of this stable point, a compensatory dynamic kicks in to drive the developing organs back toward the equilibrium. In the course of evolution, such dynamic would present a challenge to increasing the relative size of T1

legs in male *D. prolongata*. Thus, we wanted to test whether the evolutionary origin of sexual dimorphism involved an attenuation of compensatory growth control.

If the relatively higher cell proliferation in T1 compared to T2 discs in *D. prolongata* males required an attenuation of compensatory growth control, we would expect the negative correlation between segment-biased growth and the relative size of developing legs to be weaker in *D. prolongata* males compared both to *D. prolongata* females and to the males and females of *D. carrolli*, which have the ancestral leg size ratios. Surprisingly, *D. prolongata* males instead show a stronger signal of growth compensation than do females, a dimorphism that is also seen in *D. carrolli* (Figure 4B). The difference in mitotic index between segments does not correlate with overall disc size (Supplemental Figure 2), suggesting that this pattern is truly a result of developmental compensation between the organs in the two segments. Furthermore, the compensatory pattern is modified in *D. prolongata* compared to *D. carrolli*, in a sex-specific manner. The regression's isogrowth intercept (where it crosses from higher growth in T1 to higher growth in T2, marked with red circles in Figure 4B) is shifted towards a larger T1/T2 size ratio in *D. prolongata* males, compared both to *D. prolongata* females and to *D. carrolli* males (Figure 4B). Thus, evolution has maintained a conserved aspect of growth control important for developmental robustness, while modifying the target of the resulting growth dynamics to produce a major shift in adult traits.

The coordination of growth between individual organs requires information about individual disc size to be integrated with growth signaling acting at the whole-body level. We examined the variation in adult trait values to investigate whether the signals that influence global growth are implicated in the control of relative leg sizes.

Leg size increase in *D. prolongata* males is proportional across body sizes

The scaling of trait size to body size is an important pattern in animal development and shape evolution (Huxley 1932; Gould 1966; Stern and Emlen 1999). It requires the integration of body size cues with individual organ growth. A scaling pattern is apparent across species in the adult trait data, where large-bodied species have longer legs (Figure 2A). Within species, the scaling of leg size across the range of individual body sizes represents a population-level trait that may itself evolve during species divergence. In the case of increased *D. prolongata* forelegs, two distinct possibilities exist: either all individuals show the same proportional increase in leg size, or this increase occurs disproportionately depending on the individual's body size. These two possibilities have different implications for the types of global growth control that may influence intersegmental divergence in leg size. For example, organs with modified sensitivity to insulin-like peptide signaling display characteristic changes in the allometric slope, with larger individuals disproportionately gaining or losing organ size due to their relatively higher hormone titers (Mirth and Shingleton 2012).

Standard major axis regression of log-transformed data (implemented with SMATR (Warton et al. 2012)) shows that the increase in leg size relative to body size in *D. prolongata* males has occurred equally across all body sizes (Figure 5). There are no significant differences in regression slope in any species (males: Likelihood ratio 6.568, df=6, p=0.363; females: Likelihood ratio 8.837, df=6, p=0.183). In contrast, the elevation of the regression is much

higher in *D. prolongata* than in other species (Wald statistic; males: 869.3, df=6, $p < 2.22e-16$; females: 85.44, df=6, $p = 2.22e-16$). Thus, leg size increase is manifested in all individuals regardless of body size, indicating that shape evolution in this lineage is size-independent. This is in keeping with other studies of shape evolution in animals ranging from insects to mammals, in nature and in selection experiments, and in different types of organs from limbs to genitals to thorax, which indicate that the elevation of the allometric relationship is both more variable between close relatives and more responsive to selection than the slope (Voje et al. 2014).

Discussion

Animal shape evolution occurs in large part by tissue-specific growth modification (Wu et al. 2006; Lavine et al. 2015; Mirth et al. 2016). However, development is highly robust to genetic and environmental variation, the legacy of millions of years of functional constraints that favor particular size combinations (Félix and Wagner 2008). Growth control also relies on shared regulatory mechanisms, meaning that many changes that influence the relative size of one organ will have pleiotropic effects on other tissues (Sorrells and Johnson 2015). When the selective regime shifts to favor different size combinations, the evolutionary process must overcome both the robustness of the system and the possible pleiotropy of changes in growth control by integrating information conveying the sex and segment of the tissue (Christiansen et al. 2002). These constraints may bias which developmental mechanisms are most commonly manipulated by selection (Carroll 2008). We sought to use recent sex-specific shape evolution in *D. prolongata* to investigate which constraints may be impacting the evolutionary trajectory of sexual dimorphism, and which growth mechanisms have evolved to accomplish the sex-specific increase in organ size.

The ratio between first and second leg size is remarkably constant across species and sexes, with the notable exception of *D. prolongata*. The general lack of variability may reflect both a developmental constraint produced by pleiotropic mechanisms of growth control, and selective constraints imposed by locomotory integration (or, more accurately, a lack of selection to break growth coordination between segments). The constancy of relative leg size has only been violated by recent evolution in the *D. prolongata* lineage, where the origin of enlarged male forelegs overcame the constraints of both serial homology and intersexual genetic correlation. It seems likely that sexual selection generated by novel mating behavior (Setoguchi et al. 2014) has modified the selective landscape and led to the developmental changes we observe. The sexual size dimorphism exclusive to *D. prolongata* indicates that the developmental control of leg growth has evolved to incorporate segment- and sex-specific regulatory information in a novel way, enabling the response to new selective pressures acting on male morphology. However, the correlated change in relative leg size observed in *D. prolongata* females suggests that these constraints are not fully eliminated, but reach a “good enough” endpoint consistent with theoretical models describing the evolution of new dimorphisms (Lande 1980).

In principle, the earliest possible establishment of relative size difference would be in the embryonic primordia. Causing a greater number of cells to adopt leg fate would increase adult leg size even in the absence of any differences in growth rates. Although we see an

increase in the relative size of embryonic T1 leg primordia in *D. prolongata* compared to *D. carrolli*, this increase is sexually monomorphic and cannot alone explain the exaggerated male forelegs of *D. prolongata*. Instead, we found strong evidence that differential mitosis during larval growth is the major contributor to sexual dimorphism. Thus, two distinct mechanisms – cell fate specification and growth control – have responded to (presumably sex-specific) selection, but only the latter was responsible for sex-specific evolution.

The key difference that distinguishes *D. prolongata* males from other species as well as conspecific females involves a change in compensatory growth control. Although both *D. prolongata* and *D. carrolli* display a compensatory growth dynamic where relatively smaller organs undergo relatively faster growth, the “target ratio” between the T1 and T2 leg sizes is substantially higher in *D. prolongata* males compared to *D. prolongata* females or *D. carrolli* males. This sex-specific change in the equilibrium point between T1 and T2 growth rates has enabled *D. prolongata* to evolve a striking level of sexual dimorphism while maintaining normal developmental robustness and intersegmental integration.

Organ size is regulated by a combination of three interacting mechanisms: autonomous regulation, systemic growth control, and cross-talk between different organs (Shingleton and Frankino 2018). Autonomous regulation comes from the developing organ’s intrinsic size (*sensu* (Bryant and Simpson 1984)), observed phenomenologically as the size at which organs stop growing in the absence of external cues. Intrinsic size is thought to be instilled in part by gradients of patterning morphogens such as Wg and Dpp (Schwank and Basler 2010). Systemic growth control involves hormones that circulate throughout the body and stimulate or suppress growth. Common *Drosophila* growth hormones include insulin-like-peptides (ILPs), which communicate nutritional state and enable organ scaling to body size (Oldham and Hafen 2003; Tang et al. 2011), and ecdysone, which both triggers molting and stimulates growth in imaginal discs (Herboso et al. 2015; Gokhale et al. 2016). Different organs can have differential responses to the same hormone titer, depending on the expression of hormone receptors. Finally, developing organs communicate their growth state to the rest of the body to coordinate growth. This is best characterized in the context of wound healing, in which case the injured imaginal disc secretes dILP8 that interacts with neural circuits to reduce ecdysone secretion (Colombani et al. 2015). These different mechanisms interact to produce organs of appropriate size that scale properly with body size variation and are robust to developmental variation.

In this context, we can propose several potential mechanisms that could induce higher growth in T1 relative to T2 leg discs in *D. prolongata* males. First, evolution could target the mechanisms that determine the T1 leg’s intrinsic size. In this model, a shift in the parameters of organ-specific growth control would lead to changes in cell proliferation through conserved regulatory pathways, producing an organ with a larger relative size without modifying its scaling to adult body. Alternatively, evolution could increase the first leg’s sensitivity to systemic growth hormones. In this scenario, evolutionary changes involve the organ’s response to the global signals maintaining developmental coordination, as seen for example in the rhinoceros beetle horns, whose exaggerated proportions result from their hypersensitivity to ILPs (Emlen et al. 2012). This precise mechanism is unlikely in *D. prolongata*, as it produces a characteristic increase in the slope of the scaling relationship

(hyperallometric scaling (Emlen et al. 2012)) that is not consistent with our observations (Figure 5). However, increased sensitivity to other hormones that do not scale with body size, such as ecdysone, could act in an analogous manner without modifying the scaling relationship. Finally, another possible mechanism involves changes in the communication between serially homologous organs, essentially requiring the T1 disc to reach a larger relative size to satisfy the system's compensatory requirements. It is not clear whether this mechanism could produce increased proliferation in the target disc, as we observe, rather than a slowdown in the others, but this possibility deserves examination.

The evolution of relative organ size is a major contributor to morphological and functional variation across the tree of life. However, it is one of the hardest types of evolutionary change to understand at a mechanistic level, since it targets developmental processes that still remain to a large extent mysterious. Identifying the regulatory pathways that mediate shape and size evolution may improve our knowledge of basic developmental processes; conversely, a better understanding of growth regulation will help us appreciate the biases in evolutionary outcomes introduced by complex developmental controls. For instance, compensatory growth dynamics may preclude many types of mutations that influence cell proliferation from producing a consistent or selectively tolerable effect on phenotypes in nature. Further analysis of the developmental shifts responsible for the sex-specific change in relative organ size in *D. prolongata* may shed more light on the workings of the evolutionary diversity engine, while at the same time elucidating the constraints that bias its output.

Supplementary Material

Refer to Web version on PubMed Central for supplementary material.

Acknowledgments

We thank Olga Barmina for invaluable support in developing methods for dissection, fly husbandry, and immunohistochemistry, and Chelo Jane Datinguino, Mubasher Ahmed, and Nerisa Riedl for assistance in the laboratory. Susan Lott and Jeanette Natzle provided valuable comments on the manuscript and conceptual guidance at the onset of the project, along with Graham Coop, Peter Wainwright, and David Begun. Discussions with Gavin Rice, Emily Kay Delaney, Joel Atallah, David Plachetzki, Ammon Thompson, Sarah Signor, James Angus Chandler, Judy Wexler, Yige Luo, Giovanni Hanna, and Logan Blair throughout the process provided constant support and intellectual stimulation. The Olympus FV1000 confocal microscope used in this study was purchased using NIH Shared Instrumentation Grant 1S10RR019266-01. We thank the MCB Light Microscopy Imaging Facility for the use of this microscope. This work was funded by the UC-Davis Center for Population Biology Pengelley Award to DL, and by the NIH grant R35GM122592 to AK.

Literature Cited

- Andersen DS, Colombani J, and Léopold P. 2013 Coordination of organ growth: principles and outstanding questions from the world of insects. *Trends Cell Biol* 23:336–344. [PubMed: 23587490]
- Breuker CJ, Patterson JS, and Klingenberg CP. 2006 A Single Basis for Developmental Buffering of *Drosophila* Wing Shape. *PLoS One* 1:e7. [PubMed: 17183701]
- Bryant PJ, and Simpson P. 1984 Intrinsic and Extrinsic Control of Growth in Developing Organs. *Q. Rev. Biol* 59:387–415. [PubMed: 6393189]
- Carroll SB 2008 Evo-Devo and an Expanding Evolutionary Synthesis: A Genetic Theory of Morphological Evolution. *Cell* 134:25–36. [PubMed: 18614008]

- Christiansen AE, Keisman EL, Ahmad SM, and Baker BS. 2002 Sex comes in from the cold: The integration of sex and pattern. *Trends Genet* 18:510–516. [PubMed: 12350340]
- Colombani J, Andersen DS, Boulan L, Boone E, Romero N, Virolle V, Texada M, and Léopald P. 2015 *Drosophila* Lgr3 Couples Organ Growth with Maturation and Ensures Developmental Stability. *Curr. Biol* 25:2723–2729. [PubMed: 26441350]
- Copps K, Richman R, Lyman LM, Chang KA, Rampersad-Ammons J, and Kuroda MI. 1998 Complex formation by the *Drosophila* MSL proteins: Role of the MSL2 RING finger in protein complex assembly. *EMBO J* 17:5409–5417. [PubMed: 9736618]
- Duncan DM, Burgess EA, and Duncan I. 1998 Control of distal antennal identity and tarsal development in *Drosophila* by spineless-aristapedia, a homolog of the mammalian dioxin receptor. *Genes Dev* 12:1290–1303. [PubMed: 9573046]
- Emlen DJ, Warren IA, Johns A, Dworkin I, and Lavine LC. 2012 A mechanism of extreme growth and reliable signaling in sexually selected ornaments and weapons. *Science* (80-.). 337:860–864.
- Félix M-A, and Wagner A. 2008 Robustness and evolution: concepts, insights and challenges from a developmental model system. *Heredity* (Edinb). 100:132–140. [PubMed: 17167519]
- Gokhale RH, Hayashi T, Mirque CD, and Shingleton AW. 2016 Intra-organ growth coordination in *Drosophila* is mediated by systemic ecdysone signaling *Dev. Biol* 418:135–145. Elsevier. [PubMed: 27452628]
- Gompel N, and Kopp A. 2018 *Drosophila* (*Sophophora*) *carrolli* n. sp., a new species from Brunei, closely related to *Drosophila* (*Sophophora*) *rhopaloa* Bock & Wheeler, 1972 (Diptera: Drosophilidae). *Zootaxa* 4434:502–510. [PubMed: 30313176]
- Gould SJ 1966 Allometry and size in ontogeny and phylogeny. *Biol. Rev. Cambridge Philos. Soc* 41:587–640. [PubMed: 5342162]
- Held LI 1995 *Imaginal Discs: The Genetic and Cellular Logic of Pattern Formation*. Cambridge University Press.
- Herboso L, Oliveira MM, Talamillo A, Pérez C, González M, Martín D, Sutherland JD, Shingleton AW, Mirth CK, and Barrio R. 2015 Ecdysone promotes growth of imaginal discs through the regulation of Thor in *D. melanogaster* *Sci. Rep.* 5 Nature Publishing Group.
- Huxley JS 1932 *Problems of Relative Growth*. Methuen & Co. Ltd., London.
- Irvine KD, and Harvey KF. 2015 Control of organ growth by patterning and hippo signaling in *Drosophila*. *Cold Spring Harb. Perspect. Biol* 7.
- Ito Y, Harigai A, Nakata M, Hosoya T, Araya K, Oba Y, Ito A, Ohde T, Yaginuma T, and Niimi T. 2013 The role of doublesex in the evolution of exaggerated horns in the Japanese rhinoceros beetle *EMBO Rep* 14:561–567. Nature Publishing Group. [PubMed: 23609854]
- Kunkel JG 1977 Cockroach molting. II. The nature of regeneration-induced delay of molting hormone secretion. *Biol. Bull* 153:145–162. [PubMed: 889943]
- Lande R 1980 Sexual dimorphism, sexual selection, and adaptation in polygenic characters. *Evolution* (N. Y). 34:292–305.
- Lavine L, Gotoh H, Brent CS, Dworkin I, and Emlen DJ. 2015 Exaggerated Trait Growth in Insects. *Annu. Rev. Entomol* 60:453–472. [PubMed: 25341090]
- Mirth CK, Frankino WA, and Shingleton AW. 2016 Allometry and size control: what can studies of body size regulation teach us about the evolution of morphological scaling relationships? *Curr. Opin. Insect Sci* 13:93–98. Elsevier Inc. [PubMed: 27436558]
- Mirth CK, and Shingleton AW. 2012 Integrating body and organ size in *Drosophila*: recent advances and outstanding problems *Front. Endocrinol* (Lausanne). 3:1–13.
- Nijhout HF, and Emlen DJ. 1998 Competition among body parts in the development and evolution of insect morphology. *Proc. Natl. Acad. Sci* 95:3685–3689. [PubMed: 9520426]
- Nijhout HF, and Grunert LW. 2010 The Cellular and Physiological Mechanism of Wing-Body Scaling in *Manduca sexta*. *Science* (80-.). 330:1693–1696.
- O'Farrell AF, and Stock A. 1953 Regeneration and the moulting cycle in *Blattella germanica* L.: I. Single regeneration initiated during the first instar. *Aust. J. Biol. Sci* 6:485–500. [PubMed: 13093536]

- Oldham S, and Hafen E. 2003 Insulin/IGF and target of rapamycin signaling: a TOR de force in growth control. *Trends Cell Biol* 13:79–85. [PubMed: 12559758]
- Parker NF, and Shingleton AW. 2011 The coordination of growth among *Drosophila* organs in response to localized growth-perturbation *Dev. Biol* 357:318–325. Elsevier B.V. [PubMed: 21777576]
- Schindelin J, Arganda-Carreras I, Frise E, Kaynig V, Longair M, Pietzsch T, Preibisch S, Rueden C, Saalfeld S, Schmid B, Tinevez J-Y, White DJ, Hartenstein V, Eliceiri K, Tomancak P, and Cardona A. 2012 Fiji: an open-source platform for biological-image analysis. *Nat. Methods* 9:676–682. [PubMed: 22743772]
- Schneider CA, Rasband WS, and Eliceiri KW. 2012 NIH Image to ImageJ: 25 years of image analysis. *Nat. Methods* 9:671–675. [PubMed: 22930834]
- Schwank G, and Basler K. 2010 Regulation of Organ Growth by Morphogen Gradients. *Cold Spring Harb. Perspect. Biol* 2.
- Setoguchi S, Takamori H, Aotsuka T, Sese J, Ishikawa Y, and Matsuo T. 2014 Sexual dimorphism and courtship behavior in *Drosophila* *prolongata*. *J. Ethol* 32:91–102.
- Shingleton AW, and Frankino WA. 2018 The (ongoing) problem of relative growth *Curr. Opin. Insect Sci* 25:9–19. Elsevier Inc. [PubMed: 29602367]
- Singh B, and Gupta J. 1977 Two new and two unrecorded species of the genus *Drosophila* Fallen (Diptera: Drosophilidae) from Shillong, Meghalaya, India. *Proc. Zool. Soc* 30:31–38.
- Sorrells TR, and Johnson AD. 2015 Making Sense of Transcription Networks. *Cell* 161:714–723. [PubMed: 25957680]
- Stern DL, and Emlen DJ. 1999 The developmental basis for allometry in insects. *Development* 126:1091–1101. [PubMed: 10021329]
- Stieper BC, Kupershtok M, V Driscoll M, and Shingleton AW. 2008 Imaginal discs regulate developmental timing in *Drosophila melanogaster*. *Dev. Biol* 321:18–26. [PubMed: 18632097]
- Tang HY, Smith-Caldas MSB, V Driscoll M, Salhadar S, and Shingleton AW. 2011 FOXO Regulates Organ-Specific Phenotypic Plasticity In *Drosophila*. *PLoS Genet* 7:e1002373. [PubMed: 22102829]
- Tumaneng K, Russell RC, and Guan KL. 2012 Organ size control by Hippo and TOR pathways. Elsevier Ltd.
- Voje KL, Hansen TF, Egset CK, Bolstad GH, and Pélabon C. 2014 Allometric constraints and the evolution of allometry. *Evolution (N. Y.)*. 68:866–885.
- Voje KL, Hansen TF, Egset CK, Bolstad GH, and Synthesis E. n.d. Allometric constraints and the evolution of allometry. 1–47.
- Waddington CH 1942 Canalization of development and the inheritance of acquired characters. *Nature* 150:563–565.
- Wagner GP, and Lynch VJ. 2010 Evolutionary novelties.
- Warton DI, Duursma RA, Falster DS, and Taskinen S. 2012 smatr 3- an R package for estimation and inference about allometric lines. *Methods Ecol. Evol* 3:257–259.
- Wasik BR, Rose DJ, and Moczek AP. 2010 Beetle horns are regulated by the Hox gene, Sex combs reduced, in a species- and sex-specific manner. *Evol. Dev* 12:353–362. [PubMed: 20618431]
- Wu P, Jiang T-X, Shen J-Y, Widelitz RB, and Chuong C-M. 2006 Morphoregulation of Avian Beaks: Comparative Mapping of Growth Zone Activities and Morphological Evolution. *Dev. Dyn* 235:1400–1412. [PubMed: 16586442]

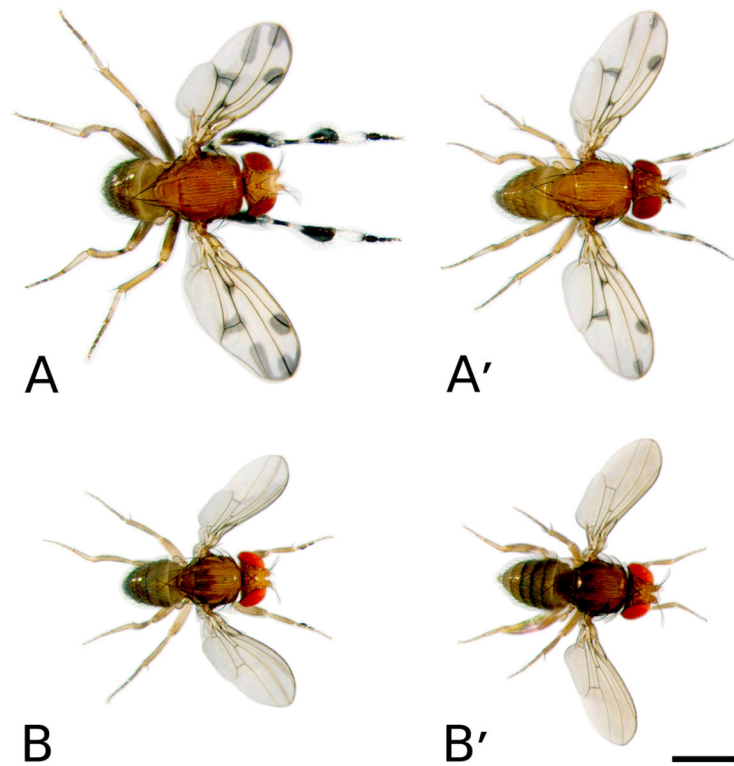


Figure 1: *D. prolongata* has a suite of recently evolved male-specific traits, most notably an increase in relative foreleg size
 Adult *D. prolongata* (A, A') and *D. carrolli* (B, B') males (A, B) and females (A', B'), showing the various sexually dimorphic traits unique to *D. prolongata*. Most noticeable is the size and banded pigmentation of the front legs in males. Other sexually dimorphic characters include wing spots, eye shape, pigmentation of the second and third legs, and an increased number of foreleg chemosensory bristles. Scale bar = 1 mm.

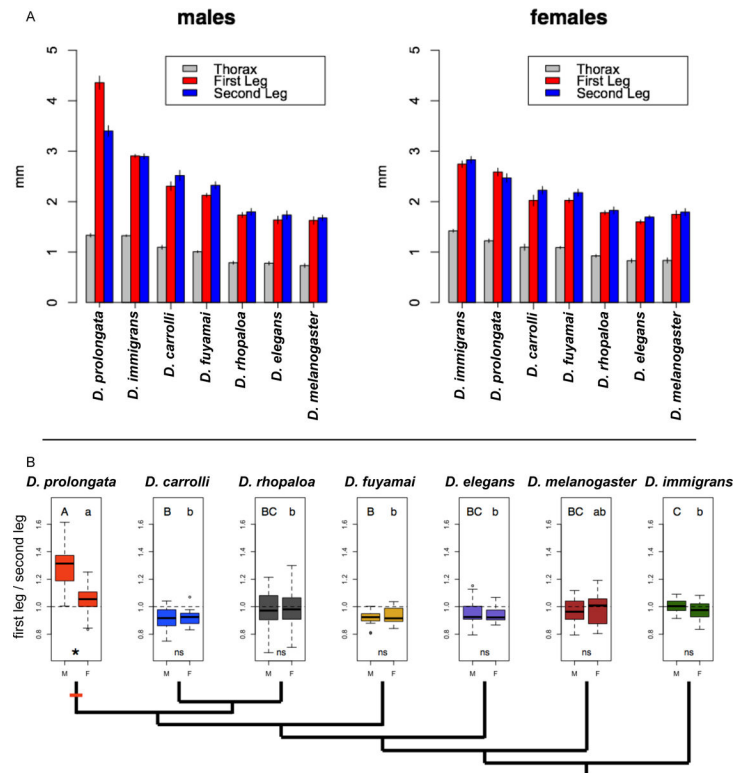


Figure 2: Sexual dimorphism of *D. prolongata* forelegs is novel and recently evolved
 Adult measures from *D. prolongata*, *D. carrolli*, *D. rhopaloo*, *D. fuyamai*, *D. elegans*, *D. melanogaster*, and *D. immigrans*. **A.** Average lengths (mm) of the thorax, first leg, and second leg of males and females from the 7 species, with standard error bars. Species are arranged within each sex by decreasing thorax length. **B.** Ratio of average first leg length to average second leg length in individual adults of both sexes from the 7 species, arranged by phylogenetic relationships as shown by the cladogram. Letters reflect groupings supported by pairwise t-tests within either sex (males upper case: *D. prolongata* vs *D. carrolli* $t=-14.44$, $df=56.98$, vs *D. rhopaloo* $t=-10.55$, $df=69.49$; females lower case: *D. prolongata* vs *D. rhopaloo* $t=-2.62$, $df=67.33$, Holm's adjusted $p=0.036$; vs *D. melanogaster* $t=-2.26$, $df=25.54$, Holm's adjusted $p=0.104$). *D. prolongata* males have the largest first-to-second leg ratio of any species. In female *D. prolongata*, the ratio is higher than in other species, but does not differ significantly from *D. melanogaster*. *D. prolongata* is the only species with statistically supported difference in leg ratio between sexes (*D. prolongata*: males; Welch $t=9.64$, $df=81.93$, Holm's $p=2.67e-14$, vs. females; $t=2.12$; *D. immigrans*: $t=2.12$, $df=38.75$, $p=0.242$). Increased first leg size and sexual dimorphism in relative leg size are unique to *D. prolongata*, and have likely evolved recently in this lineage (red tick mark on the cladogram).

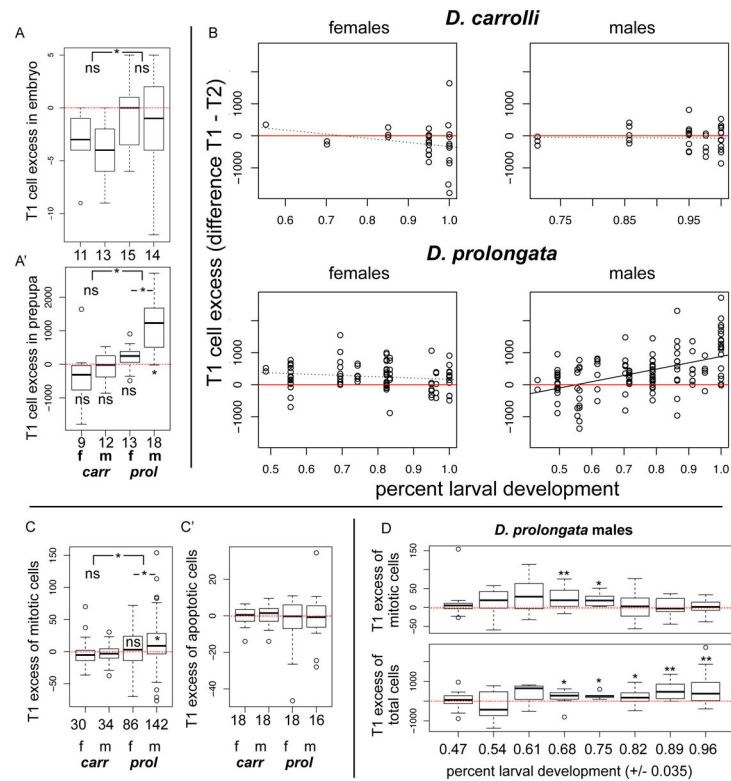


Figure 3: Larger male forelegs are produced by sex- and segment-specific increase in cell proliferation during the 3rd larval instar

A. Difference in cell number between first and second thoracic segment leg precursors in the embryo (A) and white prepupa (A') of male and female *D. carrolli* and *D. prolongata*. The y-axis reflects the difference in cell counts between T1 and T2 leg precursors, with positive values representing greater numbers of leg precursor cells in the T1 segment. Sample sizes are reported on the x-axis. In the embryonic limb primordia there is a significant effect of species (ANOVA: species $F=6.94$, $df=1$, $p=0.011$, *D. prolongata* +2.1), but no evidence of sexual dimorphism. In white prepupal discs there are significant effects of species, sex, and their interaction on the difference in cell number between T1 and T2 (ANOVA: species $F=25.8$, $df=1$, $p=6.1e-6$, *D. prolongata* +484; sex $F=14.1$, $df=1$, $p=4.7e-4$, male +229; sex*species $F=4.2$, $df=1$, $p=0.045$, prol*male +758). There is a significant difference between male and female *D. prolongata* (Welch's $t=3.62$, $df=12.28$, Holm's adjusted $p=0.019$, values averaged over 1000 bootstraps of 9 randomly subsampled observations), but not between *D. carrolli* sexes. The difference in cell number between T1 and T2 discs is significantly positive in male *D. prolongata* (male *D. prolongata*: Welch's $t=4.87$, $df=8$, Holm's adjusted $p=0.011$, averaged across 1000 bootstraps of 9 randomly subsampled observations), but not in female *D. prolongata* or either sex of *D. carrolli*. **B.** Difference in cell number between T1 and T2 discs across the third larval instar (roughly the second half of larval development) for males and females of *D. prolongata* and *D. carrolli*. Black lines depict linear regressions of cell number difference onto time point. Red lines indicate 1:1 size ratio between T1 and T2. Early in larval development, all samples have similarly sized T1 and T2 discs (values near 0, red lines). As development progresses, T1 cell bias in male *D. prolongata* increases (linear regression of difference between T1 and T2 cell counts over

relative time point: slope=1965.2, $F=41.5$, $df=123$, $p=2.4e-9$) until it reaches the level of significant difference reported in A'. **C.** Difference between T1 and T2 in the number of cells undergoing mitosis (C) or apoptosis (C') for male and female *D. prolongata* and *D. carrolli* larval leg discs from all time points. There are significant effects of species and sex, and a nonsignificant but large-effect interaction observed for differences in the number of mitoses between T1 and T2 (ANOVA species $F=7.79$, $df=1$, $p=0.006$, $prol +5.4$; sex $F=4.60$, $df=1$, $p=0.033$, male $+0.1$; $prol*male +9.3$, $p=0.25$). The number of excess mitotic cells in T1 is sexually dimorphic in *D. prolongata* but not in *D. carrolli* larval discs (Welch's $t=-2.326$, $df=200.04$, Holm's adjusted $p=0.042$). When both sexes of *D. prolongata* are tested separately, only males show a significant excess of T1 mitotic cells (Welch's $t=3.57$, $df=85$, Holm's adjusted $p=0.0049$, averaged over 10000 bootstraps of 86 randomly subsampled observations). There is no significant difference in programmed cell death, with effect sizes showing greater cell death in T1 legs of male *D. prolongata* (ANOVA species $prol -3.3$, $p=0.35$; sex male $+0.89$, $p=0.46$, $prol*male +2$, $p=0.69$). **D.** T1 excess of mitotic cells (top) and total cell count (bottom) across larval development of male *D. prolongata*. Red lines indicate no difference (1:1 size ratio). Each sample was compared to 0 by t-test: unadjusted $p < 0.05$ indicated by (*), unadjusted $p < 0.005$ indicated by (**). After Holm's adjustment for multiple tests, only (**) samples remain significantly distinct from 0. Bias in mitosis towards T1 discs varies over time, and is only significantly above 0 between 64% and 78% of larval development (by unadjusted p-value) or between 64% and 69% of larval development (after correction for multiple tests). Divergence in the size of leg discs begins to appear around 64% (unadjusted) or 85% (adjusted) of larval development and persists thereafter. The relative timing of these events is consistent with a T1 bias in mitosis producing the observed divergence between disc sizes.

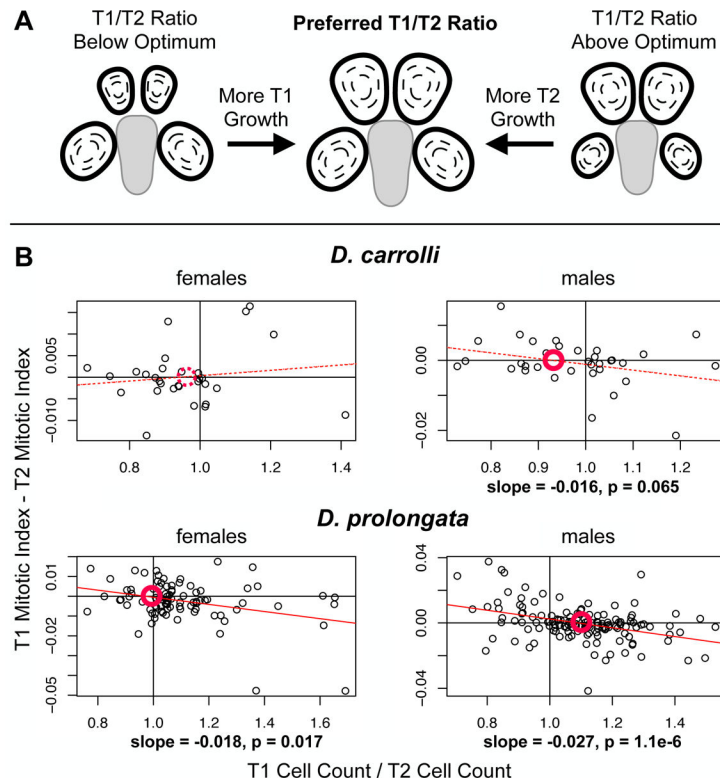


Figure 4: Intersegmental coordination of disc growth is tuned to different relative leg sizes

A. Model of compensatory growth generating T1 and T2 discs with appropriate relative sizes. When T1 discs are too small (left), or T2 discs are too small (right), higher growth in the undersized segment restores the preferred ratio. **B.** Plots show the relationship between intersegmental differences in disc size (T1/T2 cell count, x-axis) and intersegmental differences in disc growth rates (T1 – T2 mitotic index, y-axis) in males and females of *D. prolongata* and *D. carrolli*. Red lines show linear regression of the difference in the proportion of dividing cells onto the ratio of cell counts between segments. Solid red lines have slopes significantly different from zero at $p < 0.05$. Slopes and p-values are given for all regressions with $p < 0.1$. A horizontal regression line would reflect a system where the relative frequency of mitosis between the two segments does not depend on their relative sizes (no compensation). A negative regression represents a compensatory growth dynamic, where individuals with larger T1 discs have faster growing T2 discs, and *vice versa* (as depicted in Figure 4A). The T1MI - T2MI = 0 axis represents the transition from faster growth in T1 to faster growth in T2, and the x-axis intercept of this line (circled in red) represents the system's equilibrium point, i.e. the stable ratio of T1/T2 leg sizes towards which the compensatory growth is tending. A positive x-axis intercept will cause larger T1 than T2 legs, while a negative intercept will cause larger T2 legs. Growth compensation is present in both sexes of *D. prolongata*, as indicated by negative regression lines, but the size ratio at which growth equilibrates is shifted towards larger T1 legs in males compared to females.

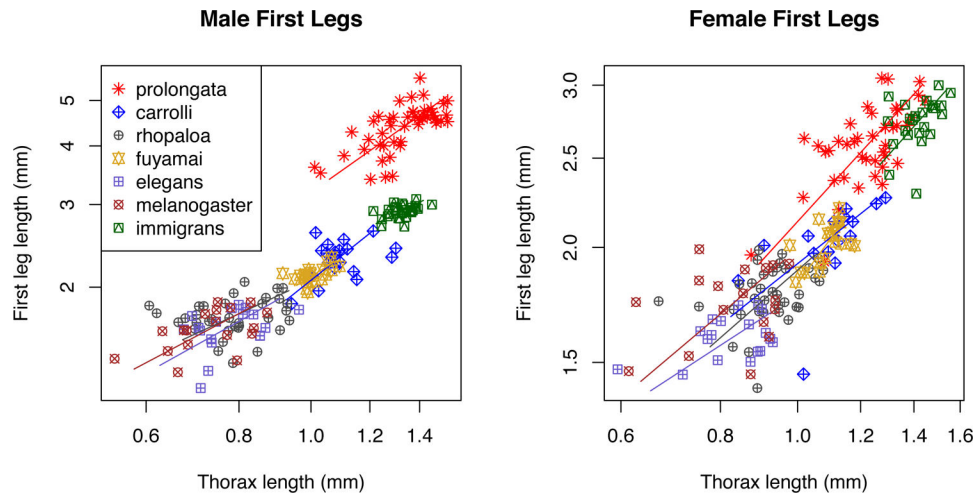


Figure 5: Increase in leg size is independent of body size

Standardized major axis regressions between first leg length and thorax length (log scale) for males and females of 7 species, showing scaling relationship of leg to body size in each sex and species. Regression slopes are not significantly different in either sex (likelihood ratio statistic; males: 6.57, $df=6$, $p=0.363$; females: 8.84, $df=6$, $p=0.183$), while differences in elevation are highly significant in both sexes (Wald statistic; males: 869.3, $df=6$, $p<2.22e-16$; females: 85.44, $df=6$, $p=2.22e-16$). In *D. prolongata* males, the shift up in intercept without a change in slope shows that all individuals, regardless of body size, gain a proportional increase in foreleg size.